A COMPARISON OF PARTICLE FILTER ALGORITHMS APPLIED TO THE HYPERTHERMIA TREATMENT OF CANCER INDUCED BY NEAR-INFRARED LASER

Bernard Lamien [1], Helcio Rangel Barreto Orlande [1], and Guillermo Enrique Eliçabe [2]

[1] Federal University of Rio de Janeiro, PEM/COPPE, CP 68503, Rio de Janeiro, RJ, 21941-972, Brazil

[2] Inst. Mat. Science and Technology (INTEMA), Univ. Mar del Plata (CONICET) - Mar del Plata, Argentina

Abstract: In this paper, the hyperthermia treatment of cancer induced by near-infrared laser light is formulated as a state estimation problem and solved with Particle Filters. The physical problem considered involves the irradiation with a laser in the near infrared range, of a multi-layered medium composed of several tissues. The layer representing the tumor is assumed to be loaded with plasmonic nanoparticles in order to enhance the hyperthermia effects and to limit such effects to the tumor region. The laser tissue interaction is modelled as a coupled radiation-bioheat transfer problem. For the solution of the inverse problem, local temperature measurements are assumed available. The inverse problem of temperature field estimation together with the fluence rate distribution is solved with three different Particle Filters, namely: the SIR Filter (Sampling Importance Resampling Filter), the ASIR Filter (Auxiliary Sampling Importance Resampling Filter) and the LIU & WEST Filter; their performance are compared in terms of solution accuracy and computational time.

Keywords: inverse problem, particle filter, hyperthermia, nanoparticles

NOMENCLATURE

D = diffusion coefficient, m
g = anisotropy factor, dimensionless
R_{sc} = specular reflection coefficient, 1/m

Greek Symbols

Φ_d = diffuse fluence rate, W/m^2
Φ_p = collimated fluence rate, W/m^2
Φ = total fluence rate, W/m^2.
ω_b = blood perfusion coefficient, 1/s
β_{tr} = transport attenuation coefficient, 1/m
β' = reduced extinction coefficient, 1/m
σ_s' = reduced scattering coefficient, 1/m
$\pi(\mathbf{a}|\mathbf{b})$ = Conditional probability of **a** when **b** is given

INTRODUCTION

State estimation problems cover a broad range of engineering applications, including telecommunication, navigation, biology, to name a few. In these kinds of problems, the available measured data is used together with prior knowledge about the underlined physical phenomena and the measuring devices, in order to sequentially produce estimates of the desired dynamic variables. This is generally accomplished in a probabilistic framework, so that, the solution of the state estimation problem consists in estimating a posterior probability density of the states through the use of the so-called Bayesian filters (Arulampalam et al., 2001, Ristic et al., 2004). As new data become available, the posterior probability density is updated, so that it reflects the current state of the system. Generally, for practical problems, the posterior probability density is not analytically tractable, and Bayesian filters from the Kalman family can be used to approximate it with a Gaussian distribution. Unlike these filters, particle filters do not rely on any local linearization or any prior assumption about the posterior probability density (Arulampalam et al., 2001, Ristic et al., 2004). Particle filters make use of importance sampling technique, which is a generalization of Monte Carlo approach for the sampling of non-explicit probability densities functions. The posterior probability density, target of the solution of the state estimation problem, is then represented by a set of samples with associated weights, referred as particles (Arulampalam et al., 2001, Ristic et al., 2004). Different particle filters algorithms can be encountered in the literature. These include, the Sampling Importance Resampling filter (SIR) and the Auxiliary Sampling Resampling filter (ASIR). The aforementioned particle filters algorithms generally failed in providing simultaneous estimates of the state variables and of the non-dynamic parameters. The problem of simultaneous estimation of state variables and of non-dynamic parameters can be handled with the LIU & WEST filter, also known as Kernel Density Particle filter. The ultimate objective of Bayesian state estimation problem is to provide better estimates of the state variables in presence of noisy data and uncertain models. Moreover, the uncertain nature of the estimates can be helpful in decision making.

Hyperthermia treatment planning or model predictive control of hyperthermia treatment can greatly benefit from the Bayesian state estimation formalism in order to provide more reliable treatment protocols. Indeed, tissues' physical properties present a large variability from an individual to another, or even under different physiological conditions. That is the input data needed for numerical simulations involving biological tissues are highly uncertain. Though tissues' physical properties are known to be uncertain, only a few works have addressed the subject (Lamien et al., 2014, Greef et al., 2011). Hyperthermia is a current research topic thanks to the recent progresses in nanotechnology. The

search for minimally invasive therapies for cancer treatment is the backbone of the use of nanoparticles in combination with traditional therapies. Indeed, the subcellular size of nanoparticles together with their appealing physical properties makes them good candidates for minimally invasive therapies. Particularly, in near-infrared photo-thermal therapy of cancer, nanoparticles with strong absorption properties are being used as photo-thermal agents in order to enhance local heat deposition in cancerous regions (Chatterjee and Krishnan, 2013, Bayatoziglu et al., 2013). Hyperthermia treatment of cancer consists in raising tumor tissues to temperatures between 42-45 ^{o}C. This treatment modality is often used as an auxiliary treatment to radiotherapy or chemotherapy, in order to improve their efficiencies. In special, near-infrared photo-thermal therapy of cancer is suggested for superficial tumors, like skin cancer, due to the limited penetration depth of laser light in tissues (Bayatoziglu et al., 2013). It is worth noting that, the near-infrared range, commonly referred in tissue optics as *optical window*, is the region of the electromagnetic spectrum in which, light penetration in tissues is optimal. For that reason, nanoparticles for photo-thermal therapy applications are designed to have strong absorption properties in the near-infrared range (Bayatoziglu et al., 2013). In addition, the excretion of the nanoparticles after the treatment is of concern and some efforts have been conducted in the development of biodegradable nanoparticles (Wang et al., 2012, Rengan et al., 2015). Several reported researches have demonstrated the selectivity and the minimally invasive feature of the use of nanoparticles for hyperthermia application (Bayatoziglu et al., 2013). However, numerical simulation is paramount in hyperthermia treatment in order to minimize damage to normal cells.

This work aims at the comparison of three particle filter algorithms, namely: the Sampling Importance Resampling (SIR) filter, the Auxiliary Sampling Importance Resampling (ASIR) filter and the LIU & WEST filter for the solution of an inverse bio-heat transfer problem of temperature field estimation resulting from the hyperthermia treatment of a subcutaneous tumor loaded with nanoparticles, by assuming available local temperature measurements from two sensors.

PHYSICAL PROBLEM AND MATHEMATICAL FORMULATION

Physical Problem

The physical problem under analysis in this work involves the hyperthermia treatment of a subcutaneous tumor, induced by an external collimated laser radiation in the form of a periodic step function, like the problem addressed in (Dombrovsky et al., 2011). The incident laser beam is uniform and perpendicular to the surface of the irradiated medium, so that the problem can be assumed as one-dimensional. The skin is modeled in terms of a multi-layered medium formed by five parallel slabs, where each slab corresponds to a specific tissue, namely (from the surface to the interior of the body): epidermis, tumor, papillary dermis, reticular dermis and fat (Dombrovsky et al., 2011). Each layer is assumed to be homogeneous and with constant optical and thermal properties.

Bio-heat Transfer Problem

The corresponding bio-heat transfer problem is governed by Pennes' equation, in which the blood perfusion and the metabolic heat generation within the tissues are taken into account, in addition to the heat source induced by the laser radiation absorption. A constant temperature boundary condition (T=T_0) is imposed at the irradiated boundary, while convective heat losses to deeper tissues beyond the computational domain is considered at the internal boundary, with a heat transfer coefficient h and with the surrounding medium at the temperature T_0. The initial temperature is uniform and equal to T_0. As in (Dombrovsky et al., 2011), the present analysis is restricted to the beginning of the treatment, so that the kinetics of the cells damage and the nonlinear behaviour of tissue properties can be neglected. The bio-heat transfer model for the one-dimensional transient problem, with the corresponding boundary and initial conditions, is then written as:

$$\rho(z)c_p(z)\frac{\partial T(z,t)}{\partial t} = \frac{d}{dz}\left(k(z)\frac{dT(z,t)}{dz}\right) + \rho_b c_{p,b}\omega_b(z)\left(T_b - T(z,t)\right) + Q_{met}(z) + Q_{laser}(z,t) \qquad (1.a)$$

$$0 < z < d \quad , \quad t > 0$$

$$T(z,t) = T_0 \quad , \quad z = 0 \ , \ t > 0 \qquad (1.b)$$

$$k(z)\frac{\partial T(z,t)}{\partial z} + hT(z,t) = hT_0 \quad , \quad z = d \quad , \quad t > 0 \qquad (1.c)$$

$$T(z,t) = T_0 \quad , \quad 0 < z < d \quad , \quad t = 0 \qquad (1.d)$$

with,

$$Q_{laser}(z,t) = \kappa(z)\Phi(z;t) \qquad (1.e)$$

where, the subscript *b* refers to blood properties, $\omega_b(s^{-1})$ is the blood perfusion rate, Q_{met} (Wm^{-3}) is the heat generation resulting from the metabolism, Q_{laser} (Wm^{-3}) is the heat source resulting from the laser absorption in the tissues, κ (m^{-1}) is the absorption coefficient and Φ (Wm^{-2}) is the laser fluence rate

Radiation Problem

The laser radiation propagation in the tissues is modelled in this work with the diffusion δ-P1 approximation (Star, 2011). At the external surface of the multi-layered medium, the incident laser radiation is assumed to be partially reflected (specular reflection), with reflection coefficient R_{sc}. The internal surfaces of the external and internal boundaries are assumed to partially and diffusively reflect the incident radiation, with reflectivity characterized by Fresnel's coefficients A_1 and A_2. Note that part of the incident radiation reaching the internal surfaces of the boundaries is transmitted to the air, in the case of the external boundary, or to deeper tissues, in the case of the internal boundary. The different interfaces between the slabs are assumed in perfect thermal contact with reflection given by Fresnel's law (Dombrovsky et al., 2011). The first two regions are assumed to contain absorbing gold nanoshells in order to increase local heat deposition. The refractive indexes (n_t) of the tissues are assumed constant and homogeneous.

The mathematical formulation of the radiation problem within the δ-P1 Approximation for the problem described above is now considered. The diffuse component of the fluence rate is given by the following boundary value problem (Star, 2011):

$$\frac{d}{dz}\left[-D(z)\frac{d\Phi_s(z;t)}{dz}+\frac{\sigma_s'(z)g'(z)}{\beta_{tr}(z)}\Phi_p(z;t)\right]+\kappa(z)\Phi_s(z;t)=\sigma_s'(z)\Phi_p(z;t) \tag{2.a}$$

$$-D(z)\frac{d\Phi_s(z;t)}{dz}+\frac{1}{2A_1}\Phi_s(z;t)=-\frac{\sigma_s'(z)g'(z)}{\beta_{tr}(z)}\Phi_p(z;t) \quad , z=0 \tag{2.b}$$

$$D(z)\frac{d\Phi_s(z;t)}{dz}+\frac{1}{2A_2}\Phi_s(z;t)=\frac{\sigma_s'(z)g'(z)}{\beta_{tr}(z)}\Phi_p(z;t) \quad , z=d \tag{2.c}$$

where

$$D=\frac{1}{3\beta_{tr}}; \quad \sigma_s'=\left(1-g^2\right)\sigma_s; \quad g'=\frac{g}{1+g} \tag{3.a,b}$$

$$A_1=\left(1+R_2\right)/\left(1-R_1\right) \tag{3.c}$$

$$A_2\approx\left(1+R_t\right)/\left(1-R_t\right) \tag{3.d}$$

with g being the anisotropy factor, σ_s the scattering coefficient, while R_1 and R_2 are the first and second moments of Fresnel's reflection coefficient, respectively.

The collimated component of the fluence rate follows the generalized Beer-Lambert's law and is given by:

$$\Phi_p(z;t)=\Phi_{0,i}(t)\exp\left(-\beta_i'\left(z-d_{i-1}\right)\right) \tag{4.a}$$

where, the subscript *i* refers to the layer and d_i the thickness of each layer. For i=1 we have:

$$\Phi_p(z;t)=\Phi_{0,1}(t)=\left(1-R_{sc}\right)E(t) \tag{4.b}$$

where $E(t)$ is the transient irradiation of the laser imposed at the external surface of the boundary. The total fluence rate is obtained by adding both diffuse and collimated components, that is,

$$\Phi(z;t)=\Phi_p(z;t)+\Phi_s(z;t) \tag{5}$$

STATE ESTIMATION PROBLEM

The *direct (forward) problem* associated with the physical problem described above consists in determining the fluence rate distribution and temperature distribution in the region, from the knowledge of initial and boundary conditions, heat sources, geometry, optical and thermophysical properties. The *state estimation problem* addressed in this work aims at the estimation of the spatial distribution of the fluence and of the transient temperature field in the multi-

layered medium, by accounting for the uncertainties on the mathematical model of the physical problem and by assuming local temperature measurements available at two locations inside the domain.

Inverse problems in which the unknowns are time-dependent are referred to as non-stationary inverse problems (Kaipio and Somersalo, 2004). On the other hand, it turns out necessary in several applications to obtain estimates of some variables from measurements obtained sequentially, in order to monitor a given process. In these situations, non-stationary inverse problems may be written in the form of evolution and observation models, in which the evolution of the unknown variables is modeled as a stochastic process (Kaipio and Somersalo, 2004, Arulampalam, 2001). The formulation of a non-stationary inverse problem in terms of evolution and observation models is referred to as a state estimation problem (Kaipio and Somersalo, 2004, Arulampalam, 2001). We consider a vector $\mathbf{x}_k$, referred to as the state vector, which contains all the state variables that describe the system at a given time instant t_k. We further assume known the state evolution model and the observation model, which are defined by the functions $\mathbf{f}_k$ and $\mathbf{h}_k$, respectively, so that we can write the evolution model and the observation model respectively as (Ristic et al., 2004):

$$\mathbf{x}_k = \mathbf{f}_k\left(\mathbf{x}_{k-1}, \boldsymbol{\theta}, \mathbf{w}_{k-1}\right) \quad , \quad k = 1, \ldots, M \tag{6.a}$$

$$\mathbf{z}_k = \mathbf{g}_k\left(\mathbf{x}_k, \boldsymbol{\theta}, \mathbf{v}_k\right) \quad , \quad k = 1, \ldots, M \tag{6.b}$$

where $\boldsymbol{\theta}$ is a vector containing all the non-dynamic parameters of the model, while $\mathbf{w}_k$ and $\mathbf{v}_k$ represent the noises in the state evolution model and in the observation model, respectively. The objective of the state estimation problem is then to obtain information about the state vector $\mathbf{x}_k$ based on the evolution and observation models defined by equations (6.a,b) (Ristic et al., 2004, Kaipio and Somersalo, 2004). In the case of the *filtering problem* addressed here, the estimation of the posterior probability density $\pi\left(\mathbf{x}_k \mid \mathbf{z}_{1:k}, \boldsymbol{\theta}\right)$ or $\pi\left(\mathbf{x}_k, \boldsymbol{\theta} \mid \mathbf{z}_{1:k}\right)$ are of interest. The later enables to account for uncertainties in the model parameters during the estimation of the state variables. We note that the probability density $\pi\left(\mathbf{x}_0 \mid \mathbf{z}_0, \boldsymbol{\theta}\right) = \pi\left(\mathbf{x}_0\right)$ or $\pi\left(\mathbf{x}_0, \boldsymbol{\theta} \mid \mathbf{z}_0\right) = \pi\left(\mathbf{x}_0, \boldsymbol{\theta}\right)$ at the initial state $t = t_0$ is assumed available, in each case.

The particle filter method is a Monte Carlo technique for the solution of state estimation problems, in which the posterior probability density function is represented by a set of random samples (particles) with associated weights. As the number of samples becomes large, the Monte Carlo characterization becomes an equivalent representation of the posterior probability density function and the solution approaches the optimal Bayesian estimate. The particle filter algorithms generally make use of an importance density, which is a probability density function proposed to represent another one that cannot be exactly computed, that is, the sought posterior density in the present case. Then, samples are drawn from the importance density instead of the actual density (Ristic et al., 2004, Arulampalam et al., 2001).

Let $\mathbf{x}_{0:k}^i$, $i = 1, \ldots, N$ be the particles with associated weights w_k^i, $i = 1, \ldots, N$ and $\mathbf{x}_{0:k} = \mathbf{x}_j$, $j = 0, \ldots, k$ be the set of all state variables up to t_k, where N is the number of particles. The weights are normalized so that $\sum_{i=1}^{N} w_k^i = 1$. In this work, the state variables are given by the fluence and the temperatures at the discrete points inside the domain that coincide with the center of finite elements used in the discretization of the direct problem. The Sampling Importance Resampling filter (SIR) and the Auxiliary Sampling Importance Resampling filter (ASIR) are used for the estimation of the posterior probability density $\pi\left(\mathbf{x}_k \mid \mathbf{z}_{1:k}, \boldsymbol{\theta}\right)$ of the state variables, while the algorithm by Liu & West, which is based on ASIR version of the particle filter, is used for the estimation of the joint posterior probability density $\pi\left(\mathbf{x}_k, \boldsymbol{\theta} \mid \mathbf{z}_{1:k}\right)$ of the state variables and of the parameters, where $\boldsymbol{\theta}$ contains the uncertain physical properties of the tissues.

The Sampling Importance Resampling filter (SIR)

In the SIR algorithm the prior density $\pi\left(\mathbf{x}_k^i \mid \mathbf{x}_{k-1}^i\right)$ is chosen as the importance density. As in this case the importance density is independent of the information conveyed by the measurements $\mathbf{z}_k^{\text{meas}}$, the state space is explored without any information of the measurements. Hence, this filter can be inefficient and sensible to outliers (Arulampalam et al., 2001). Such algorithm can be summarized in the steps presented in Tab. 1, as applied to the system evolution from t_{k-1} to t_k (Arulampalam et al., 2001, Ristic et al., 2004).

The Auxiliary Sampling Importance Resampling filter (ASIR)

The Auxiliary Sampling Importance Resampling filter was introduced in (Pitt and Shepard, 1999) as a variant of the SIR filter, in which an attempt is made to overcome the loss of diversity by performing the resampling step at time t_{k-1}, with the available measurement at time t_k (Arulampalam et al., 2001, Ristic et al., 2004). The resampling is based on some point estimate $\boldsymbol{\mu}_k^i$ that characterizes $\pi\left(\mathbf{x}_k^i \mid \mathbf{x}_{k-1}^i\right)$, which can be the mean of $\pi\left(\mathbf{x}_k^i \mid \mathbf{x}_{k-1}^i\right)$ or simply a sample of $\pi\left(\mathbf{x}_k^i \mid \mathbf{x}_{k-1}^i\right)$. If the state evolution model noise is small, then $\pi\left(\mathbf{x}_k^i \mid \mathbf{x}_{k-1}^i\right)$ is generally well characterized by $\boldsymbol{\mu}_k^i$, so

that the weights w_k^i are more even and the ASIR algorithm is less sensitive to outliers than the SIR algorithm. On the other hand, if the state evolution model noise is large, then the single point estimate $\boldsymbol{\mu}_k^i$ in the state space may not characterize well $\pi\left(\mathbf{x}_k^i \mid \mathbf{x}_{k-1}^i\right)$ and the ASIR algorithm may not be as effective as the SIR algorithm. The ASIR algorithm can be summarized in the steps presented in Tab. 2, as applied to the system evolution from t_{k-1} to t_k (Arulampalam et al., 2001, Ristic et al., 2004).

Table 1 – Sampling importance resampling algorithm (Arulampalam et al., 2001, Ristic et al., 2004)

Step 1
For i = 1,...,N draw new particles $\mathbf{x}_k^i$ from the prior density $\pi(\mathbf{x}_k\|\mathbf{x}^i_{k-1})$ and then use the likelihood density to calculate the corresponding weights $w^i_k = \pi(\mathbf{z}_k\|\mathbf{x}_k^i)w^i_{k-1}$.
Step 2
Calculate the total weight $t = \Sigma_i w^i_k$ and then normalize the weights; that is, for i = 1,...,N let $w^i_k = t^{-1}w^i_k$.
Step 3
Resample the particles as follows: Construct the cumulative sum of weights (CSW) by computing $c_i = c_{i-1} + w^i_k$ for i = 1,...,N, with $c_0 = 0$ Let i = 1 and draw a starting point u_1 from the uniform distribution U[0,N^{-1}] For j = 1,...,N Move along the CSW by making $u_j = u_1 + N^{-1}(j\text{-}1)$ While $u_j > c_i$ make $i = i + 1$ Assign sample $\mathbf{x}_k^j = \mathbf{x}_k^i$ Atribuir os pesos das amostras $w^j_k = N^{-1}$

The Liu & West filter

The algorithm of Liu & West for the particle filter is based on West's hypothesis of a Gaussian mixture for the vector of parameters $\boldsymbol{\theta}$, that is:

$$\pi(\boldsymbol{\theta}\left|\mathbf{z}_{1:k-1}\right.) \approx \sum_{i=1}^{N} w_{k-1}^i \, N(\boldsymbol{\theta}\left|\mathbf{m}_{k-1}^i, h^2\mathbf{V}_{k-1}\right.) \tag{7}$$

where $N(\cdot\left|\mathbf{m},\mathbf{S}\right.)$ is a Gaussian density with mean $\mathbf{m}$ and covariance matrix $\mathbf{S}$, while h is a smoothing parameter. Equation (7) shows that the density $\pi(\boldsymbol{\theta}\left|\mathbf{z}_{1:k-1}\right.)$ is a mixture of $N(\boldsymbol{\theta}\left|\mathbf{m}_{k-1}^i, h^2\mathbf{V}_{k-1}\right.)$ distributions weighted by the sample weights w_{k-1}^i. The kernel locations are specified by using the following shrinkage rule (Liu and West, 2001):

$$\mathbf{m}_{k-1}^i = A\,\boldsymbol{\theta}_{k-1}^i + (1-A)\overline{\boldsymbol{\theta}}_{k-1} \tag{8}$$

where $A = \sqrt{1-h^2}$ and $\overline{\boldsymbol{\theta}}_{k-1}$ is the mean of $\boldsymbol{\theta}$ at time t_{k-1}. The shrinkage factor, A, is computed as (Liu and West, 2001):

$$A = \frac{3\varepsilon - 1}{2\varepsilon} \tag{9}$$

where $0.95 < \varepsilon < 0.99$.

Table 3 summarizes the basic steps of Liu and West's algorithm (Liu and West, 2001), as applied for the advancement of the particles from time t_{k-1} to time t_k.

Table 2 – Auxiliary Sampling importance resampling algorithm (Arulampalam et al., 2001, Ristic et al., 2004)

Step 1
For i = 1,...,N draw new particles $\mathbf{x}_k^i$ from the prior density $\pi(\mathbf{x}_k|\mathbf{x}^i_{k-1})$ and then calculate some characterization $\boldsymbol{\mu}_k^i$ of $\mathbf{x}_k$, given $\mathbf{x}^i_{k-1}$. Then use the likelihood density to calculate the corresponding weights $w^i_k = \pi(\mathbf{z}_k|\boldsymbol{\mu}_k^i)w^i_{k-1}$.
Step2
Calculate the total weight $t = \Sigma_i w^i_k$ and then normalize the weights; that is, for i = 1,...,N let $w^i_k = t^{-1}w^i_k$.
Step 3
Resample the particles as follows: Construct the cumulative sum of weights (CSW) by computing $c_i = c_{i-1} + w^i_k$ for i = 1,...,N, with $c_0 = 0$ Let i = 1 and draw a starting point u_1 from the uniform distribution U[0,N^{-1}] For j = 1,...,N Move along the CSW by making $u_j = u_1 + N^{-1}(j-1)$ While $u_j > c_i$ make $i = i + 1$ Assign sample $\mathbf{x}_k^j = \mathbf{x}_k^i$ Assign sample weights $w^j_k = N^{-1}$ Assign parent $i^j = i$
Step 4
For j =1,..., N draw particles $\mathbf{x}^j_k$ from the prior density $\pi(\mathbf{x}_k|\mathbf{x}^{ij}_{k-1})$, using the parent i^j, and the use the likelihood density to calculate the corresponding weights $w^j_k = \pi(\mathbf{z}_k|\mathbf{x}^j_k) / \pi(\mathbf{z}_k|\boldsymbol{\mu}_k^{ij})$.
Step 5
Calculate the total weight $t = \Sigma_j w^j_k$ and then normalize the weights; that is, for j = 1,..., N let $w^j_k = t^{-1}w^j_k$.

RESULTS

The simulations were carried out with the thermophysical and optical properties of the tissues taken from (Çetingül and Herman, 2010, Çetingül and Herman, 2011, Tuchin, 2000); these are summarized in Tab. 4, together with the respective thicknesses of each tissue layer (Dombrovsky et al., 2011). The scattering coefficient of the tumor presented in Tab. 4 was calculated from its reduced scattering coefficient as reported in (Dombrovsky et al., 2011), by assuming an anisotropy factor of 0.9. The first and second moments of Fresnel's reflection coefficient for the air-tissue interface, with tissue refractive index n_t =1.3, were taken from (Prahl, 1988) and are respectively given by 0.565 and 0.429.

Table 5 shows the optical properties of gold nanoshells (20 nm outer diameter at the laser wavelength of λ=633 nm). The gold nanoshells were assumed to be contained only in the first two layers and their optical properties were computed assuming a volumetric fraction f_v=2x10^{-6} (%) and Mie's Scattering theory (Dombrovsky et al., 2011). Note that the absorption and scattering coefficients of tissues containing the gold nanoshells were obtained by simple summation of tissue and nanoparticle absorption and scattering coefficients. It is assumed here that only the absorption and the scattering coefficients are affected by the inclusion of the nanoparticles. The imposed laser irradiation at the surface of the body was assumed to be in the form of periodic pulses of a constant magnitude 20 kW/m^2, with duration of 10 s and period of 25 s.

For the solution of the forward problem, the finite element method was used through the COMSOL Multiphysics 4.3b commercial package. The solution obtained with the COMSOL 4.3b for the coupled radiation – bio-heat transfer problem in the multi-layered medium has been verified against the discrete ordinate method solution of the radiative transfer equation (Maurente et al., 2013).

Table 3 – Liu and West's Algorithm (Liu and West, 2001)

Step 1
Find the mean $\bar{\boldsymbol{\theta}}_{k-1}$ of the parameters $\boldsymbol{\theta}$ at time t_{k-1}.
Step 2
For $i = 1,...,N$ compute $\mathbf{m}^i_{k-1}$ with equation (8), draw new particles $\mathbf{x}^i_k$ from the prior density $\pi(\mathbf{x}_k \mid \mathbf{x}^i_{k-1}, \mathbf{m}^i_{k-1})$ and then calculate some characterization $\boldsymbol{\mu}^i_k$ of $\mathbf{x}_k$. Use the likelihood density to calculate the corresponding weights $w^i_k = \pi(\mathbf{z}_k \mid \boldsymbol{\mu}^i_k, \mathbf{m}^i_{k-1}) w^i_{k-1}$.
Step 3
Calculate the total weight $t = \Sigma_i \, w^i_k$ and then normalize the particle weights, that is, for $i = 1,...,N$ let $w^i_k = t^{-1} w^i_k$.
Step 4
Resample the particles as follows : Construct the cumulative sum of weights (CSW) by computing $c_i = c_{i-1} + w^i_k$ for $i = 1,...,N$, with $c_0 = 0$ Let $i = 1$ and draw a starting point u_1 from the uniform distribution U[0,N^{-1}] For $j = 1,...,N$ Move along the CSW by making $u_j = u_1 + N^{-1}(j-1)$ While $u_j > c_i$ make $i = i + 1$ Assign samples $\mathbf{x}^j_{k-1} = \mathbf{x}^i_{k-1}$, $\mathbf{m}^j_{k-1} = \mathbf{m}^i_{k-1}$ and $\boldsymbol{\mu}^j_k = \boldsymbol{\mu}^i_k$ Assign sample weights $w^j_k = N^{-1}$ Assign parent $ij = i$
Step 5
For $j = 1,...,N$ draw samples $\boldsymbol{\theta}^j_k$ from $N(\boldsymbol{\theta}^j_k \mid \mathbf{m}^{ij}_{k-1}, h^2 \mathbf{V}_{k-1})$, by using the parent ij.
Step 6
For j=1,...,N draw particles $\mathbf{x}^j_k$ from the prior density $\pi(\mathbf{x}_k \mid \mathbf{x}^{ij}_{k-1}, \boldsymbol{\theta}^j_k)$, by using the parent ij, and then use the likelihood density to calculate the correspondent weights $w^j_k = \pi(\mathbf{z}_k \mid \mathbf{x}^j_k, \boldsymbol{\theta}^j_k) \,/\, \pi(\mathbf{z}_k \mid \boldsymbol{\mu}^{ij}_k, \mathbf{m}^{ij}_{k-1})$.
Step 7
Calculate the total weight $t = \Sigma_j \, w^j_k$ and then normalize the particle weights, that is, for $j = 1,...,N$ let $w^j_k = t^{-1} w^j_k$.

Table 4 – Thermophysical and optical properties

Tissue	Epidermis	Tumor	Papillary Dermis	Reticular Dermis	Fat
Thickness, (mm)	0.1	0.3	0.4	0.8	2
ρ (kg/m^3)	1200	1030	1200	1200	1000
c_p (J/kg K)	3589	3582	3300	3300	3674
k (W/m K)	0.235	0.558	0.445	0.445	0.185
Q_{met} (W/m^3)	0	3680	368.1	368.1	368.4
ω_b (1/s)	0	63x10^{-4}	2x10^{-4}	13x10^{-4}	10^{-4}
κ (1/m)	800	50	15	15	2.6
σ_s (1/m)	17500	6000	17500	17500	12000

In order to avoid an inverse crime, the solution of the forward model given by equations (1.a-e) and (2.a-c) was solved with a sufficiently refined finite element mesh containing 1002 elements for the computation of the simulated temperature measurements and with 502 elements for the state estimation. As required for the solution of the state estimation problem with the Liu & West particle filter method, Gaussian prior probability densities were assumed for the different model parameters. Such densities are presented in Tab. 6, for both optical and thermophysical properties.

Table 5 – Gold nanoshells (20 nm outer diameter) optical properties ($f_v = 2x10^{-6}$ %)

κ (1/m)	σ_s (1/m)	λ_{SPR} (nm)
587	85	633

Table 6 – Prior probability densities of the optical and thermophysical properties

Physical Parameter	**Mean**	**Standard Deviation**
Absorption coefficient	κ_0	$0.03\kappa_0/2.576$
Scattering coefficient	$\sigma_{s,0}$	$0.03\sigma_{s,0}/2.576$
Anisotropy fator	g_0	$0.03g_0/2.576$
Reflectivity of the internal boundary	$R_{t,0}$	$0.03R_{t,0}/2.576$
1st moment of Fresnel reflection coefficient	$R_{1,0}$	$0.03R_{1,0}/2.576$
2nd moment of Fresnel reflection coefficient	$R_{2,0}$	$0.001R_{2,0}/2.576$
Irradiance	E_0	$0.01\ E_0/2.576$
Thermal Conductivity	k_0	$0.03k_{,0}/2.576$
Volumetric Heat Capacity	$C_{p,0}$	$0.05C_{p,0}/2.576$
Perfusion Coefficient	ω_0	$0.05\omega_0/2.576$
Metabolic Heat Source	$Q_{met,0}$	$0.05Q_{met,0}/2.576$
Heat Transfer Coefficient	$h_{conv,0}$	$0.05h_{conv,0}/2.576$

For the solution of the state estimation problem, the noise in the evolution model of the temperature was assumed as Gaussian, with zero mean and a standard deviation of 0.25 ^oC, while in the evolution model of the fluence rate the standard deviation was assumed proportional to 1/100 of the fluence at each position. Transient temperature measurements at the positions of 0.35 mm and 1.5 mm below the surface were assumed available for the inverse analysis. The measurement errors are also Gaussian, with zero mean and a constant standard deviation of 0.25 ^oC. The SIR, the ASIR and the Liu & West algorithms were used for the solution of the state estimation problem with 100 and 250 particles. The performances of these filters are compared in terms of the root mean square (RMS) error between the estimated temperatures and the exact ones. But also, in terms of the computation cost of the inverse solution for one run of each particle filter algorithm.

Figures 1(a) and (b) present the estimated temperature distributions across the domain in the first period of heating and the estimated transient temperature variation at one of the sensor position (z=0.35 mm) obtained with the three different particle filter algorithms for N=100 particles. The estimated temperatures are compared with the exact ones in the same figure. Note in Fig. 1(a) that, the estimated temperature distributions obtained at the end of heating (t=10 s) and cooling (t=25 s) of the first period are in good agreement with the exact ones. In addition one should note that, during the heating, the temperature increase in the region loaded with nanoparticles is higher than the remaining regions; that is, the addition of nanoparticles promotes a localized heating in the tumour region. In Fig. 1 (b), one can note also a good agreement between the transient variations of the estimated temperatures with the exact ones. Moreover, one can note that, when the measurements are distant from the exact ones, the estimated temperatures are still closer to the exact ones. At the graph scale, no significant differences can be seen from the estimates obtained with the three particle filter algorithms, as applied to the problem under study.

A quantitative comparison of the performance of these particle filter algorithms is presented in Tab. 7 in terms of the RMS error of the temperature for N=100 and N=250 particles. Note in this table that, the variation of the RMS error of the temperature is not significant when the number of particles was increased from N=100 to N=250 particles, for each particle filter algorithm; that is, convergence is reached for N=100 particles. One can also note that, the calculated RMS errors of the temperature decrease with depth and are larger in the regions of higher temperature. Note also that, the calculated RMS errors for the three particle filter algorithms are comparable. However, it was expected that, the Liu & West filter exhibits larger RMS errors due to the additional uncertainties of the non-dynamic parameters. This demonstrates that, the Liu & West filter performs very well for the present inverse state estimation problem. Table 8 presents a comparison of the computation cost of each particle filter algorithm. As can be seen from this table, the Liu & West algorithm presents the largest computation cost, due to the necessity to solve both radiation and bio-heat transfer problems at each time-step and for each particle in order to propagate the uncertainties of the parameters. Note also that the computation cost of the ASIR algorithm is approximately twice the one for the SIR filter. That is due to the

fact that in the ASIR filter, the state evolution model is performed twice (See Tab. 2). The computation cost of these filters also includes the cost of the process of communication between MATLAB® and COMSOL Multiphysics ®.

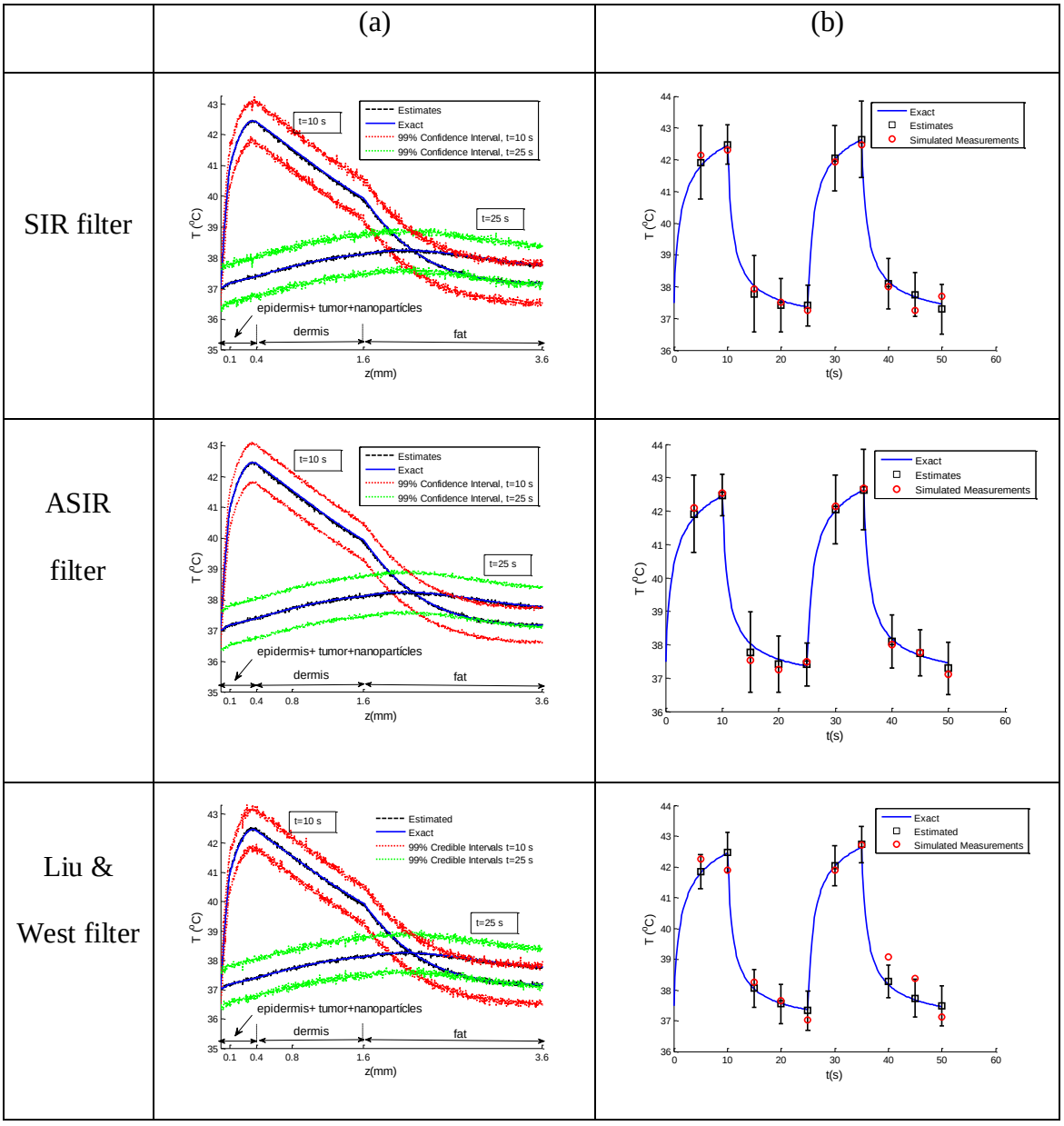

Figure 1 – (a) Exact and estimated temperature distribution at selected times with N=100 particles; (b) Comparison of the estimated and exact transient temperature variations with the temperature measurements at the sensor position z=0.35 mm, for N=100 particles

CONCLUSIONS

In this work, a coupled radiation – bio-heat transfer model was used to simulate the hyperthermia treatment of a subcutaneous tumor assumed to contain nanoparticles, and exposed to near-infrared laser light. The associated inverse problem was formulated as a state estimation problem which solution was obtained through the application of techniques chosen within the Bayesian framework, namely the Sampling Importance Resampling (SIR) filter, the Auxiliary Sampling Importance Resampling (ASIR) filter and the Liu & West's version of the particle filter. The results obtained clearly demonstrate the ability of these algorithms in providing accurate estimates of the temperature field, even under uncertainties in model's parameters and noisy measurements. Furthermore, it was shown that the Liu & West filter deals very well with the problem of simultaneous estimation of state and parameters, thus providing estimates with comparable accuracy with the SIR and the ASIR filters. However, the computational time required by the Liu & West filter for the problem addressed here is very large in comparison with the SIR and ASIR filters.

Table 7 – RMS errors of the temperature at different positions inside the domain

	Position / Number of Particles	z_1= 0.35 (mm)	p_2=0.5 (mm)	p_3=1.5 (mm)	p_4=3.0 (mm)
SIR filter	*N*=100	2.8433	2.5832	1.3207	0.8687
	N=250	2.8397	2.5802	1.3258	0.8735
ASIR filter	*N*=100	2.8758	2.5886	1.3175	0.8624
	N=250	2.8147	2.5786	1.3176	0.8670
Liu & West filter	*N*=100	2.8246	2.5799	1.2732	0.8606
	N=250	2.8330	2.5808	1.2799	0.8639

Table 8 – Computational time of the inverse problem solution

Particle filter Algorithm	Number of Particles	CPU time
SIR	100	1 h 13 min
SIR	250	3 h 05 min
ASIR	100	2 h 30 min
ASIR	250	6 h 15 min
Liu & West	100	4 h 58 min
Liu & West	250	11 h 57 min

ACKNOWLEDGMENTS

The financial support provided by CNPq, CAPES and FAPER is greatly appreciated.

REFERENCES

Arulampalam, M. S., Maskell, S., Gordon, N., et al., 2001, ''A Tutorial on Particle Filters for Online Nonlinear/Non-Gaussian Bayesian Tracking'', IEEE Transactions on Signal Processing, Vol. 50, No 2, pp. 174-188.

Bayatoziglu, T., Kheradmand, S., Tullius, K. T., 2013, ''An Overview of Nanoparticle Assisted Laser Therapy'', Int. J. of Heat and Mass Transf, v. 67, pp. 469-486.

Çetingül, M. P., Herman, C., 2010, ''A Heat transfer model of skin tissue for the detection of lesions: sensitivity analysis'', Physics in Medicine and Biology, Vol. 55, No. 19, pp. 5933-5951.

Çetingül, M. P., Herman, C., 2011, ''Quantification of the thermal signature of a melanoma lesion'', Int. J. Therm. Sci., Vol. 50, No. 4, pp. 421-431.

Chatterjee, D., Krishnan, S., 2013, ''Gold nanoparticle – mediated hyperthermia in cancer therapy,'' In S. Cho and S Krishnan, Eds., Cancer Nanotechnology, Boca Raton, CRC Press, pp. 171-182.

Dombrovsky, L. A., Timochenko, V., Jackson, M., et al., 2011, ''A Combined Transient Thermal Model for Laser Hyperthermia of Tumors with Embedded Gold Nanoshells'', Int. J. of Heat and Mass Transfer, Vol. 54, pp. 5459–69.

Greef, D.M., Kok, H.P., Correia, D., Borsboom, P.P, Bel, A., Crezee, J., 2011, ''Uncertainty in Hyperthermia Treatment Planning: The Need for Robust System Design'', Phys. Med. Biol., 56, pp.3233-3250.

Kaipio, J. P. and Somersalo, E., 2004, ''Statistical and Computational Inverse Problems'', Applied Mathematical Sciences 160, Springer-Verlag.

Lamien, B., Orlande, H.R.B., 2014, ''State Estimation Problem in Hypertthermia Treatment of Tumors Loaded with Nanoparticles, Proceedings of the 15th International Heat Transfer Conference, August 10-15, 2014, Kyoto, Japan.

Liu, J., West, M., ''Combined Parameter and State Estimation in Simulation-Based Filtering'', In Doucet, A., de Freitas, N., Gordon, N., (Eds.), *Sequential Monte Carlo Methods in Practice*, New York, Springer-Verlag, (2001).

Maurente, A., Lamien, B., Orlande, H. R. B., et al., ''Analysis of the P1-Approximation for the Radiative Heat Transfer in Skin Tissues Loaded with Nanoparticles'', Proc. of 22th Brazilian Congress of Mechanical Engineering Engineering, pp. 931-940, (2013).

Pitt, M. Shephard, N., 1999, ''Filtering via Simulation: Auxiliary Particle Filters'', Journal of American Statistical Association, v. 94, n. 446, pp. 590-599

Prahl, S. A., 1988, ''Light Transport in Tissue'', Doctoral Dissertation, The University of Texas, Austin.

Rengan, A.K., Bukhari, A.B., Pradhan, A., Malhotra, R., Banerjee, R., Srivastava, R., De, A., 2015, ''In Vivo Analysis of Biodegradable Liposome Gold Nanoparticles as Efficient Agents for Photothermal Therapy of Cancer'', Nano Lett, Vol. 15, No. 2, pp.842-848.

Ristic, B., Arulampalam, S., Gordon, N., 2004, ‘’Beyond the Kalman Filter’’, Artech House, Boston.
Star W.M., 2011, “Diffusion Theory of Light Transport’’. In Welch, A. J., Van Gemert, J.C.M. Eds, Optical-Thermal Response of Laser irradiated Tissue, 2 ed., Dordrecht Heidelberg London New York, Springer.
Tuchin, V., 2000, ‘’Tissue Optics, Light Scattering Methods and Instruments for Medical Diagnosis’’, Washington: SPIE
Wang, Q., Xie, L., He, Z., Di, D., Liu, J., 2012, ‘’Biodegradable Magnesium Nanoparticle-Enhanced Laser Hyperthermia Therapy’’, Int. J. Nanomedicine, Vol.7, pp.4715-4725.

RESPONSIBILITY NOTICE

The authors are the only responsible for the material included in this paper.